Enhanced functional properties of biodegradable Polyvinyl alcohol /carboxymethyl cellulose (PVA/CMC) composite films reinforced with L-alanine surface modified CuO nanorods

Yamanappagouda Amaregouda
Rani Channamma University
Kantharaju Kamanna (kk@rcub.ac.in)
RCUB https://orcid.org/0000-0002-4696-5401
Tilak Gasti
Karnatak University Dharwad
Vijay Kumbar
Maratha Manadal college of pharmacy

Research Article

Keywords: CuO NPs, chemically surface modification, Microwave, Nanocomposite, Antioxidant, Cytotoxicity

Posted Date: September 29th, 2021

DOI: https://doi.org/10.21203/rs.3.rs-918116/v1

Version of Record: A version of this preprint was published at Journal of Polymers and the Environment on January 17th, 2022. See the published version at https://doi.org/10.1007/s10924-022-02377-6.

Enhanced functional properties of biodegradable Polyvinyl alcohol /carboxymethyl cellulose (PVA/CMC) composite films reinforced with L-alanine surface modified CuO nanorods

Yamanappagouda Amaregouda[1], Kantharaju Kamanna[1]*, Tilak Gasti[2] and Vijay Kumbar[3]

[1]*School of Basic Sciences: Department of Chemistry, Rani Channamma University, Vidyasangama, P-B, NH-4, Belagavi -591156, Karnataka.*
Tel: +91(0831)-2565203; Fax: +91-(0831)-2565240
**Corresponding author:* E-mail: kk@rcub.ac.in
[2]Department of Chemistry, Karnatak University, Dharwad – 580003, India
[3]Maratha Mandal's Central Research Laboratory, Belgavi-590010

Abstract

Herein, we described novel biogenic preparation of the CuO nanorods and its surface modification with L-alanine amino acid accelerated by microwave irradiation. The effect of surface functionalized CuO nanorods on the polyvinyl alcohol/carboxymethyl cellulose film physico-mechanical properties were investigated through various characterization techniques. The tensile strength was improved from 28.58±0.73 MPa to 43.40±0.93 MPa, UV shielding ability and barrier to the water vapors were highly enhanced when PVA/CMC matrices filled with 8 wt% of CuO-L-alanine. In addition, the prepared films exhibited acceptable overall migration limit and readily undergoes soil burial degradation. Nevertheless, CuO-L-alanine incorporated films showed potent antioxidant activity against DPPH radicals and had high antibacterial activity against *Staphylococcus aureus and Escherichia coli*, and antifungal activity against *Candida albicans* and *Candida tropicalis*. Furthermore, the nanocomposite films showed negligible cytotoxic effect on HEK293 and Caco-2 cell lines. In these contexts, the developed nanocomposite films can be implementing as an active food packaging material.

Keywords: CuO NPs, chemically surface modification, Microwave, Nanocomposite, Antioxidant, Cytotoxicity

Introduction

The environmental impact on the solid waste from petroleum-based packaging materials can be overcome by replacement of biodegradable polymer materials [1]. Hence, development of nontoxic and environment-friendly films with antimicrobial properties for food packaging application are highly promising [2]. PVA (polyvinyl alcohol) is a highly biocompatible and nontoxic synthetic polymer with high water solubility due to the hydroxyl group, and it has been used in food, membrane, medicine, and other materials manufacturing. These wider applications prompted material scientist to exploit further by designing novel composite materials [3]. PVA is flammable and quickly ignited, it is important to improve the PVA's flame retardancy as well as mechanical qualities for various application, including textiles, furniture, adhesives, and packaging materials[3]. To overcome this limitation, researchers described alternative technique involving blending of PVA with other polymers derived from natural or synthetic such as chitosan [4], polycaprolactone [5], PLA [6], starch [7], PVA and CMC [8]. But, PVA and CMC polymeric

blends are of particular interest because they are compatible and form a hydrogen bond easily [9]. Several reported work highlighted the blending of CMC with PVA resulted improvement of the PVA properties[10]. Saadieh et al, developed biopolymer blend electrolytes based on PVA/CMC film and author shows the non-Debye characteristics where no single relaxation time has observed [11]. Ghorpade et al, designed polymeric blend films based on citric acid cross-linked CMC/PVA for the extended release of the water-soluble medicine [12]. Miao et al, prepared a negatively charged nanofiltration membrane based on PVA/CMC-Na composite using interfacial polymerization[13]. Muppalla et al, used the casting method to prepare PVA/CMC films containing clove oil as active packaging for ground chicken meat [14]. Agarwal et al, developed PVA/Polyethylene oxide/CMC membrane for the drug delivery application by freeze-drying and solvent casting [15]. The blending of CMC with PVA can enhance the biodegradable properties. Despite this, some physical properties of the PVA/CMC blend are poor than synthetic polymers derived from the petroleum resources. Recently several research teams have reported the great potential of CuO nanostructure for enhancing PVA/CMC blend performance in terms of mechanical, thermal, and barrier properties leading to the production of greener nanocomposites [16]. The CuO nanostructures found promising nanocomposite production, owing to their large specific surface area, wide availability, biocompatibility, and biodegradability, which may offer great opportunities to develop environmental friendly structural composites [17]. CuO nanostructures have been used as a suitable filler to strengthen the mechanical property of the polymeric nanocomposites [18]. However, only a few report on the application of CuO nanostructure in the food packaging areas are reported in the literature [19]. The CuO nanostructures with a high ratio of surface area to volume tend to agglomerate, which severely impedes their application. Thus, chemical and physical surface modification on the nanostructures can be utilized effectively to prevent agglomeration and increase their dispersibility. L-Alanine is an amino acid with suitable biodegradability, biocompatibility, nontoxic and eco-friendly properties, that obtained by hydrolysis of proteins [20]. The L-alanine can therefore be selected in the present work for chemical and physical surface modification of the CuO nanostructure.

In the present work, for the first time we have reported CuO nanorods required for the composite film preparation using novel greener route employing WEMPA (water extract of mango peel ash) is described. The composite films required for this work is prepared by reported casting method and are characterized by FESEM, EDX, powder XRD, TGA, DSC, FT-IR, and UV-Vis spectroscopy. We introduced L-alanine for the chemically surface modification of CuO nanorods by microwave approach. The surface modification was confirmed by the FESEM, EDX, XRD, FT-IR, TGA, DSC, and UV-Vis spectroscopy. Then, modified CuO nanorods were introduced into the PVA/CMC blend for the preparation of PVA/CMC/CuO-L-alanine NCs. Finally, the prepared nanocomposites were characterized for mechanical, thermal, morphology, water vapor transmission, moisture retention capacity, overall migration, and soil burial degradation. Further, *in vitro* cytotoxicity, antibacterial, antifungal, and antioxidant properties were investigated.

Material and methods

Materials

Mango fruits were purchased at a local market in Belagavi, Karnataka. India. PVA (MW: 60,000 to 1,25,000 g mol^{-1}) and CMC (MW: 250,000 g mol^{-1}) were obtained from HIMEDIA, Cupric nitrate trihydrate [Cu $(NO_3)_2.3H_2O$] was obtained from Merck, and L-Alanine was obtained from Sigma-Aldrich, India. The ethanol and acetic acid were supplied by SD Fine Chemicals in India. The 2,2–diphenyl–1–picrylhydrazyl was supplied by Sigma–Aldrich in India (DPPH). Double distilled water was utilized throughout the experiment. All other reagents and chemicals employed were analytical grade and did not require further purification.

Preparation of WEMPA

Mango fruits were collected from local market Belagavi, Karnataka. The fruit peel is removed from the pulp, and washed in distilled water before being dried in the sun light for about 4 to 5 days. The dried peels are burned on a Bunsen flame to obtain ash, the obtained 10 gm of the ash was placed in a 500 mL conical flask, and added 100 mL of deionized water. The mixture is agitated for about 2 h at room temperature, then filtered, and the filtrate is known as water extract of mango peel ash (WEMPA) [21]. The pH of the extract solution is 10.8 and it is in alkaline.

CuO nanorods preparation

Initially, 2 mmol of copper nitrate trihydrate [Cu $(NO_3)_2.3H_2O$, 0.48 g] was dissolved in 20 mL of double distilled water and agitated using a magnetic stirrer for 15 min at room temperature. Afterward, 60 mL of prepared WEMPA solution (pH value 10.8) was added drop-wise to the 20 mL copper nitrate trihydrate at 60 °C with continuous stirring (250 rpm) for 4 h. After the addition of WEMPA, the solution became blackish jelly (black precipitate), which confirms the formation of CuO NRs (rod-shaped nanoparticles were confirmed by SEM morphology). This black precipitate is washed with double distilled water 2–3 times and then again washed with ethanol 3–4 times. Furthermore, the obtained black precipitate was dried at 80 °C for 24 h in a hot air oven followed by calcination at 700 °C for 6 h.

Modification of CuO nanorods

Typically, 0.035 g of CuO nanorods in 5 mL ethanol was sonicated for 15 min and was added to 0.2 g L-alanine amino acid (4 mmol) in double distilled water/ethanol solvents (4:1). The mixture was transferred to the RB flask, followed by heating in the custom made microwave oven up to 120 °C for 40 min with the output power of 700 W [22]. After the RB flask was naturally cooled to room temperature, modified CuO nanorods were isolated by centrifugation and washed with double distilled water and ethanol. Then, the product was dried at 80 °C in a vacuum.

Fabrication of PVA, PVA/CMC, PVA/CMC/CuO-L-alanine amino acid NCs films

Initially, 2 g of PVA and 0.5 g of CMC were dissolved separately in 100 mL and 50 mL of water respectively. Both the solutions were mixed and stirred for a while, thereafter different weight percentage (0, 2, 4, 6, and 8 wt%) CuO-L-alanine NRs dispersed in water *via* ultrasonication was added to it and stirred for 24 h, and further sonicated to achieve homogeneity. The resulting solution was casted on a dried petridish and allowed to dryness for 5h at 50°C. The dried films were peeled off and stored in a zip lock pouch until further study. The neat PVA film was prepared according to the above mentioned protocol without using CMC and CuO nanorods [23].

UV-Vis Spectroscopy

The formation of CuO nanorods, surface modification of CuO nanorods, and the light barrier properties (opacity, transparency, and % transmittance) of the prepared nanocomposite films were investigated using UV–Vis spectroscopy (Shimadzu, UV-1800, USA). The film sample (4 ×1 cm) was placed in a sample cell and the spectrum was recorded in the wavelength range of 200-800 nm using air as a standard reference. Three measurements were recorded for the same sample and results were expressed in mean standard deviation (n=3). The opacity and transparency of the nanocomposite films were calculated using Eq. (1) and Eq. (2).

$$Opacity = \frac{Abs_{500}}{b} \qquad (1)$$

Where $Abs_{500}$the absorbance at 500 nm and b is is the thickness of the film (nm).

$$Transparency(T_{600}) = \frac{-\log(\%T_{600})}{b} \qquad (2)$$

Where %T is the percentage transmittance at 600 nm and b is the film thickness in nm

Fourier transform infrared (FT-IR) analysis

The FT-IR spectra of the films were acquired in the range of 4000-400 cm^{-1} using an attenuated total reflectance – Fourier transform infrared (ATR FT-IR) spectrophotometer (Thermo Scientific, Nicolet iZ10). This technique was used to analyze the structural changes in the nanocomposite films.

X –Ray diffraction (XRD) analysis

The X-ray diffraction (XRD) analysis of the prepared CuO NRs and film samples were carried out using Rigaku Miniflex, Diffractometer, the reflection mode with Cu Kα radiation at 30 kV, 10 mA and a scan rate of 2% min and scan range of 10º to 80° (2θ).

Scanning Electron Microscopy (SEM) and energy dispersive X-ray (EDX)

SEM with an energy dispersive X-rays (EDX) spectrometer of VEGA3, TESCAN (CZECH REPUBLIC) was used to examine the surface morphology of the nanocomposite films. Before further treatment, the samples were covered with a thin palladium/platinum conductive coating. A sputter coating was used to produce the layer. A secondary electron detector with a 30 kV accelerating voltage was used to view the surface of the sample.

Mechanical properties

Mechanical strength of the prepared nanocomposite films is measured for the tensile strength (Ts), elongation at break (Eb), and young's modulus (E) using computer-based DAK testing machine (UTM) according to ASTM D882–91 standard. The films were cut into rectangular pieces with a dimension of (0.5 x 0.71 cm) and the tests were carried out at a 1 mm/min crosshead speed and a gauge length of 5 cm.[24]. The thickness of each sample is considered for the testing and average reading was taken. The average thickness of the prepared films are observed 0.009 ± 0.002 cm.

Thermal Analysis

The thermal stability and decomposition temperature of the film samples were evaluated using thermogravimetric analysis (TGA) (TA-SDT650 instruments, USA). The film sample (4–4.5 mg) was heated in the temperature range 25–600 °C at an incremental rate of 10 °C /min under the nitrogen atmosphere (50 mL/min). TA Instruments, USA, was used to perform the differential scanning calorimetry (DSC). The 1.5–2.0 mg of the film sample was sealed in an aluminum crucible and heated in an inert nitrogen atmosphere (50 mL/ min) from 25 to 400 °C at a heating rate of 10 °C /min.

Water vapor transmission rate (WVTR)

The prepared films were evaluated for their water vapor transmission rate (WVTR) using a method described in the literature [25] with certain changes. Briefly, 10 mL of DDI water was placed into a glass bottle with an inner diameter of 29.5 mm, and the mouth of the glass bottle was wrapped with prepared films and tightened with Teflon tape to conduct the test. The initial bottle's weight (W_i) was recorded before heating, and it was placed in a preheated hot air oven at 40 °C for 24 hours. The sample bottle was taken out of the oven after 24 hrs and weighed (W_f) again, WVTR was calculated using Eq. (3).

$$WVTR = Water\ vapor\ transmission\ rate = [W_i - W_f/A] \times T \qquad (3)$$

where A is the area of the mouth of the bottle and T = 24 h.

Moisture retention capability

The moisture retention capacity (MRC) of the prepared films were measured using ASTM D570-98, before and after drying in an oven at 105±2 °C for 24 h. The weight of the film samples was calculated using Eq. (4) for the MRC (%).

$$\text{MRC}\ (\%) = \text{Moisture retention capacity}(\%) = [W_i/W_f] \times 100 \qquad (4)$$

Where W_i and W_f are the weight of the films before and after drying respectively.

Surface wettability test

A water contact angle meter was used to assess the surface wettability of the prepared films using the sessile drop technique (Kyowa Interface Science Co. Ltd., Tokyo). The film sample (2×2 cm) was mounted on the specimen holder, and a micro syringe used to drop 2 µL of distilled water onto the film surface. A high–resolution camera was used to capture the contact angle between the film surface and the water droplet picture, and preloaded software was used to determine the static water contact angle. The water contact angle was measured in triplicate at different places on the same film sample and given as mean ±SD.

Soil Burial Degradation (SBD)

The SBD of the prepared nanocomposite films was tested using a slight modification of the previous reported method [26]. Briefly, the film sample (1.415 × 1.415 cm) was dried at 80 °C and weighed. The dry samples weighed are buried in a black soil at a depth of 10 cm, and 10 mL of water added every day up to 30 days. After 30 days of treatment, the buried films were carefully

removed, rinsed with water, and dried at 80 °C. The dried weights of the degraded samples were measured and calculated the percentage degradation using Eq. (5).

$$SBD\ (\%) = \text{Soil burial degradation}\ (\%) = \frac{Initial_{wt} - Final_{wt}}{Initial_{wt}} \times 100 \qquad (5)$$

Overall Migration Rate

The food compatibility of the prepared nanocomposite films was determined gravimetrically by calculating the total migration rate of the film contents into food simulants in accordance with IS: 9485 (1998) guidelines. The film sample was immersed in each beaker containing 30 mL DDI water, 3% acetic acid, and 50% ethanol solutions and kept in a hot air oven at 40 °C for 10 days. The samples were dried and weighed again after 10 days. The films overall migration limit into the food simulants was given in mg/dm^2.

Antioxidant Activity

The DPPH (2,2-diphenyl-1-picrylhydrazyl) method was used to determine the antioxidant activity of the prepared films based on their free radical scavenging activity by reported protocol. Briefly, 2 mL (1 mMol) of DPPH in methanolic solution and 1 mL each of five different concentrations (20, 40, 60, 80, and 100 g/mL) of each sample solution were mixed and incubated at room temperature for 30 minutes. These incubated sample mixtures were exposed to UV–Vis spectrophotometer to record absorption values at 517 nm. Ascorbic acid (AA) was employed as a standard reference and a blank DPPH solution was used as a control. Three tests were done for the same sample and results were reported in mean ± SD. The scavenging activity of the DPPH IC_{50} was calculated using Eq. (6).

$$DPPH\ radical\ scavenging\ activity\ (\%) = \frac{Abs_{control} - Abs_{sample}}{Abs_{control}} \times 100 \qquad (6)$$

Antibacterial and antifungal activity

In order to investigate the antibacterial and antifungal properties of the prepared nanocomposite films, we have selected to test in four different food pathogenic bacteria including Gram-positive (*S. aureus*), Gram-negative bacteria (*E. coli*), and fungi (*C. albicans* and *C. tropicalis*). Firstly, nutrient broth culture was prepared by inoculating pure colonies of the test organisms followed by incubation for 24 h. In brief, 10 mg of the film sample was dissolved in 10 µL of DMSO as a stock solution. For antibacterial test, 1.5 µL brain heart infusions (BHI) agar and 10 µL of each *E. coli* and *S. aureus* suspension was taken in a test tube and mixed well, to this 100µL of film samples from stock solution was added and mixed gently. Test tube was inoculated at 37 ℃ for 24 h, after 24 h colonies were counted as colony-forming units per mL (CFU/mL). For an antifungal (*C. albicans* and *C. tropicalis*) activity studies, the above-stated method was employed by using sabotaged dextrose agar (SDA) instead of BHI and control is prepared as above without the sample.

***In vitro* cytotoxicity assay**

The cell viability of the prepared films was tested through MTT (3-(4,5-dimethylthiazol-2-yl) -2,5-diphenyl tetrazolium bromide) assay according to the reported method [27]. Briefly, HEK293

cells were seeded on a 96 well plates and were placed in a CO_2 incubator at 37°C for 24 hours. The films of different composition were placed on to the plate and three replications for each film was analyzed. As per manufacturer's instructions, 100µL of freshly prepared media containing 10 µL of MTT solution (5mg/mL in PBS) used to replace the previous media after 24 hours. The plates were again incubated on the aforementioned condition for 4 hours. After this stage, the formazan crystals in the well were dissolved with 0.1 mL of DMSO. The optical density of the MTT formazan product was measured with absorbance recorded in a 570 nm wavelength range using microplate reader. Antimycotic 100x used as a negative standard. The cell viability was calculated using the following equation (7), where OD is the optical density which is measure of the absorbance of the sample.

$$Cell\ viability\ (\%) = \frac{Mean\ OD\ of\ sample}{Mean\ OD\ of\ Negative\ control}\ X\ 100 \qquad (7)$$

Statistical analysis

Origin–9 program employed one-way analysis of the variance statistical analysis (Origin Lab USA). The tests were carried out in triplicates, with the average standard deviation (n = 3) being reported.

RESULT AND DISCUSSION

UV–Visible Spectroscopy

Figure.1a appended UV-Vis absorption spectrum of WEMPA showed at 310 nm, CuO nanorods prepared shows the absorption peaks at 317 nm and functionalized CuO-L-alanine exhibited 310 nm peaks, which are most likely attributed to the Surface Plasmon Resonance (SPR) of CuO and CuO-L-alanine semiconductor excitation. UV light resistance is strictly required to be considered when polymeric films are considered in packaging, especially in the case of light-sensitive food products [28, 29]. Although PVA/CMC blend is widely applied as a packaging material, but its poor UV resistance needs to be improved to broaden the application sector. CuO-L-alanine showed excellent UV barrier properties (Fig. 1b) and also observed the transmittance (Fig. 1c) of the nanocomposite films containing CuO-L-alanine in the UV region (for instance 320 nm) reached a value below 2%, it confirmed how these nanocomposites could be used in the specific fields, where UV protection is needed. On the other hand, PVA and PVA/CMC blend films without CuO-L-alanine were found more transparent (lower transmittance value at 550 nm) than those coupled with CuO-L-alanine. This reduction in the transmittance of both UV and visible light is associated with the interaction of CuO-L-alanine with the PVA/CMC blend and responsible for the compact and higher polymeric chain network preventing the passage of UV light in the case of CuO-L-alanine blend film. Kanmani et al. (2014) reported that, when nanoparticles are dispersed homogeneously on the polymeric matrix, it leads to a decrease in the light transmission [30]. In this work, the prepared film PCC-4 showed the best UV barrier properties due to the higher concentration of the CuO-L-alanine. The transparency and opacity of the films were also depicted in Fig 1d. The opacity measurement is a well-established method for determining film transparency. The higher the transparency, the lower the opacity value, and vice versa. The PVA/CMC film was less opaque and more transparent, when CuO-L-alanine is added to the PVA/CMC blend the film transparency is substantially reduced, and nanocomposite films becomes

more opaque. The influence of CuO-L-alanine continued to diminish the transparency of the nanocomposite films. According to Salari et al. (2018), nanoparticles had a greater influence on the film's transparency [31], and results obtained for the prepared NCs films could also be used as an effective UV barriers.

FT-IR Spectroscopy

Figure 2 displays FT-IR spectra of the CuO nanorods and CuO/L-alanine functionalized. The CuO nanorods prepared using agro-waste revealed the absorption maxima at 641, 1382, 1630, and 3441 cm^{-1}. The CuO bending vibration could be responsible for the band at 641 cm^{-1}. The bending vibrations of the –OH group linked to the Cu atom were attributed to the peaks detected at 1630 and 1382 cm^{-1}. The large band at 3441 cm^{-1} could be attributed to the stretching vibrations of the –OH group adsorbed water molecules on CuO nanorods. A new band at 2204 cm^{-1}, which is attributable to the C-H stretching of the L-alanine amino acid. The carboxylic acid C=O stretching vibration is responsible for the broad band at 1695 cm^{-1}. The bending vibration of the N-H group, stretching vibration of the C-N group, and C-H of alkyl groups, respectively, are attributed absorption bands at 1550, 1462, and 1382 cm^{-1}, which can also be related to the carboxylate anion (COO-) asymmetric and symmetric stretching bonds. The band at 640 cm^{-1} is assigned to CuO bending vibration, while the band at 595 cm^{-1} is due to the N-H group ($-NH^{3+}$) bending vibration. The FT-IR spectra of CuO/L-alanine nanorods revealed that L-alanine molecules were chemically bonded rather than just adsorbed on the CuO surface. The infrared spectra of pure PVA, PVA/CMC, and PVA/CMC/CuO-L-alanine composite films are shown in Figure 2. At 3000–3500 cm^{-1} a characteristic –OH stretching band, and 2920 cm^{-1}, CH_2 stretching band of PVA, PVA/CMC was identified. The -CH vibrational bands were found at 1312 and 1250 cm^{-1}, respectively, while the C-C stretching band was found at 835 cm^{-1}. At 1695 and 1082 cm^{-1}, the C=O bending bands on the PVA and PVA/CMC backbone, respectively were observed. The L-alanine functionalized nanocomposite spectra showed changes in peak troughs, illustrating the effect of CuO-L-alanine nanofiller inclusion on PVA/CMC bonding. The hydrogen bonding between CuO oxygen and the –OH group of PVA/CMC, where the broad band of 3000–3500 cm^{-1} is pushed towards the lower wavenumber [32]. The vibration of the CuO and N-H bending ($-NH^{3+}$) in the spectra of PVA/CMC/CuO-L-alanine amino acid NCs, which indicates the CuO/L-alanine nanorods presence might be attributed to the absorption band about 464 and 605 cm^{-1}.

XRD

The XRD method can be used to determine the crystal phase and crystallinity of the prepared films. Figure 3 shows the XRD pattern of the CuO, surface modified CuO, PVA, PVA/CMC, and PVA/CMC/CuO-L-alanine NCs with various loadings (2, 4, 6, and 8 wt%). The XRD pattern's diffraction peaks are all well matched with JCPDS data (45-0937) demonstrating that pure typical monoclinic structure of CuO NRs were effectively synthesized. Diffraction peak associated with CuO and L-alanine were observed in the CuO-L-alanine XRD pattern, L-alanine is associated with the diffraction peaks at $2\theta = 29.22$ and 31.79°, and CuO is related to the other diffraction peaks (JCPDS 45- 0937) [33]. It was confirmed that, the surface of the CuO NRs has been modified with L-alanine, and observed the crystalline phase structure of it not changed. Pure PVA exhibited a semicrystalline structure due to the strong interaction hydrogen bonding at the chain polymer and

showed two peaks at about 2θ = 19.5° (major crystalline peak) and 2θ = 41° with low intensity [34]. The broad peak in the XRD pattern of PVA is slightly shifted to a lower value of 2θ (20°) and the weak intense peak to a higher value of 2θ (40.5°) when 0.5 % CMC is added (Fig 3). This confirms the blend's structural changes and demonstrated CMC interacts strongly with PVA. The CuO-L-alanine peaks were prominent in the XRD patterns of the PVA/CMC NCs films. The intensity of the peak related to the CuO-L-alanine is enhanced with increasing content of the modified CuO in the PVA/CMC blend that indicated NCs prepared.

Morphology of CuO, CuO-L-alanine, PVA, PVA/CMC and PVA/CMC/CuO-L-alanine NCs films

The morphology of the CuO and CuO-L-alanine functionalized was studied by the FE-SEM technique. The FE-SEM image of the CuO and CuO-L-alanine are presented in Figure 4a and Figure 4c respectively. The FE-SEM images of CuO indicated that the CuO consists of a large number of fine nanorods, as shown in the Figure 5c & 5f. The modified CuO nanorods with L-alanine showed no aggregation. The morphology of the CuO nanorods was completely changed after the functionalization of L-alanine amino acid onto the CuO surface were thicken and stacked exhibited thick-edge and layered structures. In addition, EDX was used to analyze the elemental profiles of the CuO nanorods and CuO-L-alanine nanorods, and elemental mappings were carried out to illustrate the elemental distribution of each component (C, O, N and Cu) significantly in Fig. 4a and Fig. 4c respectively. The results indicate that Cu and O exist in the simple CuO nanorods, and C, N, O, and Cu elementals exist in the modified CuO-L-alanine are dispersed uniformly [35]. The FE-SEM photographs of the PVA, PVA/CMC, and PVA/CMC/CuO-L-alanine nanocomposite films are appended in Figure 5a-5f. It is observed that, the FE-SEM images of PVA and PVA/CMC films are smooth, compact, and homogeneous surfaces. The FE-SEM photographs of PVA/CMC/CuO-L-alanine nanocomposite films demonstrated that modified CuO nanorods are uniformly distributed into the polymer matrix without conglomeration (Figure 5c- Figure 5f). Furthermore, in the FE-SEM photographs of PVA/CuO-L-alanine nanocomposite films observed with number of CuO-L-alanine increases led improved appearance of the CuO-L-alanine image (2 wt% to 8 wt%).

Mechanical property

To investigate the effect of mechanical properties of the modified CuO nanorods on PVA/CMC, mechanical tests including E-modulus, tensile strength, and elongation at break were carried out [35]. Figure 6a depicts the tensile stress-strain curves of the pure PVA, PVA/CMC, and films containing 2, 4, 6, and 8 wt% CuO-L-alanine NRs with the results are summarized in Table 1. Particle size and morphology, particle loading and distribution, the polymer matrix, and interfacial adhesion between modified CuO and polymer are all aspects that can affect the mechanical properties of the NCs. In comparison to PVA/CMC, the tensile strength and E-modulus (Fig. 6b) of NCs are higher, which could be owing to strong interfacial adhesion between CuO-L-alanine and PVA/CMC, and homogeneous dispersion of the modified CuO within the PVA/CMC matrix.

Thermal property analysis

The thermal stability of the CuO nanorods and functionalized CuO-L-alanine were investigated by TGA analysis (Figure 7a). Five percentage weight loss is observed at the temperature 500 °C, which can be attributed to the removal of physically adsorbed water on CuO nanorods. The CuO-

L-alanine functionalized exhibited two steps weight loss in the temperature range of below 140 °C is due to the physically adsorbed water and weight loss in 140-500 °C is reasonably associated with desorption of chemically bound alanine in the CuO-L-alanine. The amount of the L-alanine attached on the CuO surface was determined based on CuO and CuO-L-alanine char yield difference at 500 °C. The calculated L-alanine content was found to be about 23 wt%. Thermal decomposition behavior of the PVA, PVA/CMC and PVA/CMC/L-alanine NCs is depicted in Figure 7a. Also, the resulting TGA data for thermal degradation are summarized in Table 2. TGA curve of the pure PVA and PVA/CMC polymer revealed three weight loss regions. Generally, the weight loss at 100-200 °C can be due to the evaporation of the adsorbed water in PVA and PVA/CMC chains. At the second stage at 200-400 °C, the weight loss could be related to the polymer dehydration and formation of a polyacetylene-like structure. In the last stage, at 400-500 °C the decomposition of the PVA and PVA/CMC main chain release CO_2 gas and formation of the oxides. In TGA curve, we observed that PVA/CMC blend film thermally stable than neat PVA film, this is due to the strong interaction between the PVA and CMC. TGA curve of the PVA/CMC/CuO-L-alanine NCs showed three weight loss regions. The first region at temperature of 100-220 °C is due to the evaporation of weakly physical bound water and the evaporation of residual solvents. At the second stage, the weight loss region of 200-400 °C is corresponded to the decomposition of the L-alanine amino acid, the polymer dehydration and formation of a polyacetylene-like structure. The third degradation stage at 400-550 °C corresponded to the decomposition of main chain of PVA/CMC. The pure PVA and PVA/CMC films showed 7% and 9% residue decompose at 500 °C respectively, while the weight percent remaining after major degradation at 450 °C for NCs (2, 4, 6 and 8 wt%) is higher than the control PVA/CMC blend. PVA/CMC/CuO-L-alanine NC 2 wt%, PVA/CMC/CuO-L-alanine NCs 4 wt%, PVA/CMC/CuO-L-alanine NC 6 wt% and PVA/CMC/CuO-L-alanine NC 8 wt% had 12%, 15%, 19% and 22% residue loss at 500 °C. According to this result PVA/CMC/CuO-L-alanine NCs have higher thermal stability than the pure PVA/CMC and NC 8 wt% could be optimized amount.

Further, the thermal properties are evaluated using DSC for the CuO, CuO-L-alanine, neat PVA, PVA/CMC, and PVA/CMC nanocomposites are shown in Fig. 7b and the glass transition temperature (T*g*) values were given in Table 2. In Figure 7b, we can see that the T*g* value of CuO-L-alanine is higher than CuO, because CuO-L-alanine is more crystalline than CuO. The prepared neat PVA and PVA/CMC blend films were shown in a single T*g* value which suggests that the complete miscibility of the PVA and CMC. In order to determine the effect of CuO-L-alanine on thermal properties of the PVA/CMC blend, DSC thermograms were applied and thermal parameters, namely glass transition temperature (Tg) of the films were measured and tabulated in Table 2. As can be seen, the Tg was increased with the increase of the CuO-L-alanine concentration from 2 wt% to 8 wt% in the PVA/CMC blend. The Tg of PVA/CMC nanocomposites is affected by the dispersion of CuO-L-alanine on PVA/CMC blend, hydrogen bonding, and interaction of polymer chains and CuO-L-alanine [36]. The formation of strong hydrogen bonds between CuO-L-alanine and PVA/CMC blend can reduce the segmental mobility of polymer chains and therefore increase of the Tg.

Water vapor transmission rate (WVTR)

Food packaging materials should be able to prevent moisture from the outside environment entering into the film. The food packaging films with low WVTR values have been determined to be acceptable. The structure of the polymers and the interaction between additives and polymers

determine the water vapor transmission rate of the prepared films [37]. Figure 8a shows the WVTR values of neat PVA, PVA/CMC, and PVA/CMC/CuO-L-alanine composite films. The WVTR of the PVA and PVA/CMC was found to be 40.04 ± 1.34 and 40.93 ± 3.45 $g.m^{-1}$·h respectively. This increase is due to the more hydrophilic nature of the CMC. As it can be seen WVTR of PVA/CMC was reduced with increasing CuO-L-alanine concentrations. The film containing higher concentration of CuO-L-alanine (PCC-4) showed lower WVTR. CuO NRs containing L-alanine, which acts as a bridge between the PVA and CMC polymer chains *via* intermolecular H–bonding promoting the formation of a close network structure that reduces the water absorption resulting in a lower WVTR. The number of free hydrophilic hydroxyl groups is also reduced as a result of the formation of H–bonds between CuO-L-alanine and the polymer matrix, which reduces the interaction with water molecules.

Moisture retention capacity (MRC)

The loss of water vapors from the films is determined by moisture retention capability. Moisture migration must be controlled to maintain the texture, flavor, and general quality of the packaged goods. A high or its own amount of moisture may aid to maintain product quality, and also extending the shelf life, depending on the food product. The moisture retention capacity of neat PVA, PVA/CMC, and PVA/CMC/CuO-L-alanine composite films is shown in Figure 8a. The MRC values of the prepared films ranged from 85 to 87 %. The PVA/CMC film showed higher MRC value (87.53 %) than neat PVA and PVA/CMC/CuO-L-alanine composite films. It is observed that, MRC of the PVA/CMC was reduced with increasing CuO-L-alanine concentrations. This might be attributed to the high surface area of CuO-L-alanine and its strong interaction with PVA/CMC chains leading to lower availability of the free hydroxyl groups and, consequently, a reduction in hydrophilicity and MRC value [38]. However, PVA/CMC/CuO-L-alanine films having good moisture retention capabilities. The values were in accordance to the moisture level need to be maintained for foods and fruits i.e., 78%-95% (ITC, 2012).

Soil burial degradation

Nowadays it's necessary to prepare biodegradable packaging material to reduce the environmental garbage problems. Figure 8a shows the degradation of prepared nanocomposite films after burial in soil. In the soil burial test, there was often two-step degradation. One is that the adsorption of water molecules by the film surface causes an increase in the swelling rate of the film, allowing microorganisms to grow on it. Another phase is an enzymatic breakdown, which occurs when bacteria damage the polymeric network [39]. The SBD of pure PVA was found to be 40.27 ± 2.52 % this is because of the hydrophilic surface of PVA, and the SBD of PVA/CMC was found to be 46.71 ± 1.63 % this is due to the blending of two different molecule types resulting in the structure deformation and making more hydrophilic networks. SBD of PCC-1, PCC-2, PCC-3, and PCC-4 was found to be 49.32 ± 2.41, 50.13 ± 1.93, 50.89 ± 1.83 and 51.46 ± 1.34. respectively. This enhancement in the soil degradability was due to the presence of L-alanine content which provides a higher carbon source for microbes that were get activated by the addition of water and interrupt the polymer interactions.

Surface wettability test

The water contact angle (WCA) is used to determine the hydrophilicity and hydrophobicity of the film surface. WCA > 90° and < 90° were considered to be hydrophobic and hydrophilic respectively [40]. WCA of the prepared nanocomposite films was shown in Fig. 8b. All the prepared nanocomposite films were found to be hydrophilic (WCA < 90°). The WCA of pure PVA was found to be 64.53 ± 3.21° this is because of the hydrophilic surface of PVA, and WCA of PVA/CMC was found to be 63.43 ± 1.39° this shows that the PVA/CMC film has a hydrophilic surface this hydrophilicity is due to the strong interaction between the more numbers of –OH groups present in the CMC and PVA. WCA of PCC-1, PCC-2, PCC-3, and PCC-4 was found to be 68.25 ± 1.53, 68.93 ± 1.74, 69.18 ± 1.85 and 69.87 ± 1. respectively. This increase in the WCA is due to the higher concentration of CuO-L-alanine providing more –OH groups which sufficiently H-bonded with the PVA/CMC film matrix and repelled the suspended water molecules on the film surface resulting in an increased WCA value. Similar reports were observed for cocoa extract-induced polylactide films.

Overall migration rate

Food compatibility is the most important parameter to evaluate the release of contents from the polymer matrix in food packaging. The overall migration of all prepared samples was represented in Fig. 9. It is found that the overall migration of all the film samples shows higher in the 50% Ethanol compared to 3% acetic acid and double distilled water simulants. Due to the less hydrophilicity of nanocomposite films overall migration rate is lower than that of the controlled PVA/CMC film. The CuO-L-alanine incorporated PVA/CMC nanocomposite films showed overall migration rates within the acceptable limit of 10 mg/dm^2. The reduction in the overall migration rate for the three simulants (Double distilled water, 3% acetic acid, and 50% ethanol) was due to the ability of CuO-L-alanine to restrict the release of contents into the surrounding media [36]. The CuO-L-alanine that occupy the vacant space of polymer matrix held via intermolecular hydrogen bonding, and resist the migration of contents into the food simulants. Further, this may due to the in-situ complexation of the PVA, CMC, and L-alanine components and less hydrophilic properties of the nanocomposite films. These results were consistent with the WCA measurements

In-vitro antioxidant activity

DPPH radicals have been widely used to evaluate the ability of the active compounds as free radical deactivators or hydrogen donors in order to evaluate the antioxidant activity. The DPPH free radical scavenging assay (%) and half-maximal inhibitory concentration (IC50) of prepared films are presented in Fig. 10a. The ability to deactivate these radicals by pure PVA, PVA/CMC, and PVA/CMC films incorporated with CuO-L-alanine was determined by DPPH methods. The control PVA and PVA/CMC films presented disabling radical activity of 2.2 ± 1.0% and 4.9 ± 4 μmol. g^{-1} for the DPPH assays, respectively. As expected, the incorporation of CuO-L-alanine in the films caused a significant increas in the antioxidant activity of PVA/CMC films. This is due to the presence of L-alanine which is responsible for antioxidant activity in the nanocomposite film [41]. Strong, moderate, and weak antioxidant activity are indicated by IC50 values of 10–50, 50–100, and > 100 g/mL, respective. When compared to the control PVA/CMC film, all prepared composite films have lower IC50 values (Figure 10b). The films PCC-1, PCC-2, PCC-3, and PCC-4 had lower IC50 values than conventional ascorbic acid, indicating that these composite films have significant antioxidant activity, but PVA film had moderate activity (IC50 > 50 g/mL).

Antibacterial and Antifungal activity

For a food packaging material, it is desirable to have antimicrobial properties to minimize the microbial growth in food [42]. Here the antibacterial activities of neat PVA, PVA/CMC and PVA/CMC/CuO-L-alanine films were assessed against Gram-negative E. coli and Gram-positive S. aureus by total colony count method and the log CFU/mL of each film was plotted (Fig. 11a and 11b) [43]. The neat PVA film, as well as the PVA/ CMC films, exhibit very low antibacterial activity against the test organisms. Meanwhile, films containing CuO-L-alanine have shown characteristic antibacterial activity towards both S. aureus and E. coli bacteria and as the concentration of the CuO-L-alanine increases in the nanocomposite films the antibacterial activity of both S. aureus and E. coli was increased, it suggested that the activity depended on the concentration of CuO-L-alanine in the nanocomposite films. This is due to the content of nanosized copper oxide in the polymer blend generate reactive oxygen species (ROS), which interact with the cell membrane of bacteria to enter into the cell that results in the inhibition of bacterial cell growth due to the disturbance in the cell membrane that might lead to death. Furthermore, Copper oxide nanoparticles also cause DNA and protein damage, prevent biofilm production, damage proton efflux pumps, and oxidize bacterial cells' cellular substances.

Antifungal activity of films was also evaluated by using the colony count method log CFU/mL of each film was plotted (Fig. 11c and 11d). The results revealed that the PVA and PVA/CMC films had extremely little growth inhibition against Candida albicans and Candida tropicalis. On other hand, films containing CuO-L-alanine have very good growth inhibition against the activity both C. albicans and C. tropicalis fungus and as the concentration of the CuO-L-alanine increases in the nanocomposite films the antifungal activity of both C. albicans and C. tropicalis was increased, it was also suggested that the activity depended on the concentration of CuO-L-alanine in the nanocomposite films. The content of nanosized copper oxide in the polymer blend is responsible for antifungal activity. The mechanism mainly involves cell membrane damage, disruption of energy metabolism, generation of oxidative stress due to reactive oxygen species formation, and inhibition of transcription.

Cytotoxicity evaluation

In the assessment of the prepared films as antibacterial and antifungal agents, the determination of cytotoxicity is important [44]. MTT assay was used to investigate the cytotoxicity of pure PVA, PVA/CMC and PVA/CMC films containing different content of CuO-L-alanine. HEK293 (Human embryonic kidney 293) and Caco-2 (Cancer coli-2) cells were used as sample test cells. As shown in Fig. 12a-12b, the cells treated with pure PVA and PVA/CMC film showed very good viability. The PVA/CMC film showed better biocompatibility than pure PVA. Moreover, the PVA/CMC film containing CuO-L-alanine exhibited cell viability in the range of 84–90% revealing non-toxicity towards both HEK-293 cell and Caco-2 cells. The cell viability of PVA/CMC/CuO-L-alanine film was improved with the increase in CuO-L-alanine concentration from 2 wt% to 8 wt%. The result was expected because in a previous study, the cell viability of chitosan copolymers was found to be higher when the alanine-grafted chitosan content was increased [45]. The IC_{50} value is the most important parameter to determine the cytotoxicity analysis of the NC films against cell lines. If the IC50 is > 90 µg/ml, the compound is classified as not cytotoxic. If the IC50 is between 2 and 89 µg/ml, the compound is classified as moderately cytotoxic. If the IC50 is < 2 µg/ml, the compound is classified as cytotoxic. In our work all the prepared films shows

IC_{50} is > 90 µg/ml against both HEK293 cells and Caco-2 cells, result indicate that the prepared films are not cytotoxic.

CONCLUSION

In this study, the microwave strategy was used for chemically modifying CuO nanorods with L-alanine amino acid aiming to improve their properties. Different amounts of modified CuO nanorods (2, 4, 6 and 8 wt%) were introduced into the PVA/CMC blend for the preparation of PVA/CMC/CuO-L-alanine NC films. The XRD result indicated that monoclinic crystalline CuO was successfully synthesized. According to the XRD results, TGA, DSC and FE-SEM images the modification process had no effect on crystalline phase and morphological structure. FE-SEM images showed that the CuO and the modified CuO presented a rod-like morphology. The surface morphology of NCs was examined using FE-SEM analysis and images confirmed homogeneous dispersion of modified CuO in the PVA/CMC blend. The FE-SEM, EDX, TGA confirms the surface modification of CuO. PVA/CMC/CuO-L-alanine nanocomposite films were prepared by solution casting method and their properties were examined. The prepared films indicated strong antimicrobial activity against both Gram-negative (E. coli) and Gram-positive (S. aureus) bacteria and also the prepared films showed strong antifungal activity against C. tropicalis and C. albicans fungus. The cytotoxicity of the composite films was studied in HEK293 cell and Caco-2 cell using an MTT assay. The results showed that the cell viability was more than 90% which clearly manifested the non-cytotoxicity effect of nanocomposite films. All CuO-L-alanine incorporated NC showed enhanced antioxidant activity by DPPH scavenging assay. The physical properties of the films including mechanical testing, WVTR, soil burial degradation and moisture retention capability were also measured. The mechanical properties were enhanced and WVTR decreased with the incorporation of CuO-L-alanine. The films were found to possess high moisture retention capability which are favorable for fresh fruits and vegetables with high respiration rate. The light barrier, overall migration, and WCA (77.07%) properties of PVA/ CMC films were significantly improved by the influence of CuO-L-alanine. The thermal stability of the reinforced composite films having CuO-L-alanine was higher than the neat PVA and PVA/CMC blend films. SEM and XRD analysis indicate that the CuO-L-alanine are dispersed homogenously within the PVA/CMC blend. Based on the enhanced mechanical, antimicrobial and antioxidant properties, we envisage to exploit the developed films for food packaging as well as for biomedical application such as wound dressings. However, when considering the high safety aspects of the released CuO-L-alanine, L-alanine is non-toxic and is also useful for food preservation and can therefore be used as direct food packaging materials.

CRediT authorship contribution statement

Yamanappagouda Amaregouda: Conceptualization; Data curation; Formal analysis;
Methodology; Resources; Software; Roles: Writing – original draft;
Writing – review & editing.
Tilak Gasti: Data curation, formal analysis; Role: Writing original draft.
Kantharaju Kamanna: The corresponding author; Investigation;
Supervision; Validation; Visualization; Role: Review & editing.
Vijay Kumbar: Data curation, formal analysis; Role: Writing original draft.

Declaration of competing interest

None.

Acknowledgement

Authors are thankful to UGC for the award of Major Research Project and VGST, Govt. of Karnataka for SMYSR award and K-FIST-Level-II for financial support to KK.

Appendix A. Supplementary data

Supplementary data to this article can be found online at

Reference

1. Ncube LK, Ude AU, Ogunmuyiwa EN, et al (2020) Environmental impact of food packaging materials: A review of contemporary development from conventional plastics to polylactic acid based materials. Materials 13:1–24. https://doi.org/10.3390/ma13214994
2. Zhong Y, Godwin P, Jin Y, Xiao H (2020) Biodegradable polymers and green-based antimicrobial packaging materials: A mini-review. Advanced Industrial and Engineering Polymer Research 3:27–35. https://doi.org/10.1016/j.aiepr.2019.11.002
3. Aslam M, Kalyar MA, Raza ZA (2018) Polyvinyl alcohol: A review of research status and use of polyvinyl alcohol based nanocomposites. Polymer Engineering and Science 58:2119–2132. https://doi.org/10.1002/pen.24855
4. Yu Z, Li B, Chu J, Zhang P (2018) Silica in situ enhanced PVA/chitosan biodegradable films for food packages. Carbohydrate Polymers 184:214–220. https://doi.org/10.1016/j.carbpol.2017.12.043
5. Huang D, Hu Z De, Ding Y, et al (2019) Seawater degradable PVA/PCL blends with water-soluble polyvinyl alcohol as degradation accelerator. Polymer Degradation and Stability 163:195–205. https://doi.org/10.1016/j.polymdegradstab.2019.03.011
6. Li HZ, Chen SC, Wang YZ (2014) Thermoplastic PVA/PLA blends with improved processability and hydrophobicity. Industrial and Engineering Chemistry Research 53:17355–17361. https://doi.org/10.1021/ie502531w
7. Abdullah ZW, Dong Y (2019) Biodegradable and water resistant poly(vinyl) alcohol (PVA)/starch (ST)/glycerol (GL)/halloysite nanotube (HNT) nanocomposite films for sustainable food packaging. Frontiers in Materials 6:1–17. https://doi.org/10.3389/fmats.2019.00058
8. Darbasizadeh B, Fatahi Y, Feyzi-barnaji B, et al (2019) Crosslinked-polyvinyl alcohol-carboxymethyl cellulose/ZnO nanocomposite fibrous mats containing erythromycin (PVA-CMC/ZnO-EM): Fabrication, characterization and in-vitro release and anti-bacterial properties. International Journal of Biological Macromolecules 141:1137–1146. https://doi.org/10.1016/j.ijbiomac.2019.09.060
9. Youssef AM, Assem FM, El-Sayed HS, et al (2020) Synthesis and evaluation of eco-friendly carboxymethyl cellulose/polyvinyl alcohol/CuO bionanocomposites and their use

in coating processed cheese. RSC Advances 10:37857–37870. https://doi.org/10.1039/d0ra07898k

10. Jain N, Singh VK, Chauhan S (2017) A review on mechanical and water absorption properties of polyvinyl alcohol based composites/films. Journal of the Mechanical Behavior of Materials 26:213–222. https://doi.org/10.1515/jmbm-2017-0027

11. Saadiah MA, Samsudin AS (2018) Electrical study on Carboxymethyl Cellulose-Polyvinyl alcohol based bio-polymer blend electrolytes. IOP Conference Series: Materials Science and Engineering 342:0–11. https://doi.org/10.1088/1757-899X/342/1/012045

12. Ghorpade VS, Dias RJ, Mali KK, Mulla SI (2019) Citric acid crosslinked carboxymethylcellulose-polyvinyl alcohol hydrogel films for extended release of water soluble basic drugs. Journal of Drug Delivery Science and Technology 52:421–430. https://doi.org/10.1016/j.jddst.2019.05.013

13. Miao J, Zhang R, Bai R (2015) Poly (vinyl alcohol)/carboxymethyl cellulose sodium blend composite nanofiltration membranes developed via interfacial polymerization. Journal of Membrane Science 493:654–663. https://doi.org/10.1016/j.memsci.2015.07.031

14. Behnezhad M, Goodarzi M, Baniasadi H (2019) Fabrication and characterization of polyvinyl alcohol/carboxymethyl cellulose/titanium dioxide degradable composite films: An RSM study. Materials Research Express 6:. https://doi.org/10.1088/2053-1591/ab69cb

15. Gupta B, Agarwal R, Sarwar Alam M (2013) Aloe vera loaded poly(vinyl alcohol)-poly(ethylene oxide)-carboxymethyl cellulose-polyester nonwoven membranes. Journal of Biomaterials and Tissue Engineering 3:503–511. https://doi.org/10.1166/jbt.2013.1111

16. El Sayed AM, El-Gamal S, Morsi WM, Mohammed G (2015) Effect of PVA and copper oxide nanoparticles on the structural, optical, and electrical properties of carboxymethyl cellulose films. Journal of Materials Science 50:4717–4728. https://doi.org/10.1007/s10853-015-9023-z

17. Katsumiti A, Thorley AJ, Arostegui I, et al (2018) Cytotoxicity and cellular mechanisms of toxicity of CuO NPs in mussel cells in vitro and comparative sensitivity with human cells. Toxicology in Vitro 48:146–158. https://doi.org/10.1016/j.tiv.2018.01.013

18. Rao JK, Raizada A, Ganguly D, et al (2015) Enhanced mechanical properties of polyvinyl alcohol composite films containing copper oxide nanoparticles as filler. Polymer Bulletin 72:2033–2047. https://doi.org/10.1007/s00289-015-1386-4

19. Hoffmann TG, Peters DA, Angioletti BL, et al (2019) Potentials nanocomposites in food packaging. Chemical Engineering Transactions 75:253–258. https://doi.org/10.3303/CET1975043

20. Dandare SU, Ezeonwumelu IJ, Shinkafi TS, et al (2021) L-alanine supplementation improves blood glucose level and biochemical indices in alloxan-induced diabetic rats. Journal of Food Biochemistry 45:1–9. https://doi.org/10.1111/jfbc.13590

21. Hiremath PB, Kamanna K (2019) A Microwave Accelerated Sustainable Approach for the Synthesis of 2-amino-4H-chromenes Catalysed by WEPPA: A Green Strategy. Current Microwave Chemistry 6:30–43. https://doi.org/10.2174/2213335606666190820091029

22. Mallakpour S, Nezamzadeh Ezhieh A (2017) Preparation and characterization of chitosan-poly(vinyl alcohol) nanocomposite films embedded with functionalized multi-walled carbon nanotube. Carbohydrate Polymers 166:377–386. https://doi.org/10.1016/j.carbpol.2017.02.086

23. Sarwar MS, Niazi MBK, Jahan Z, et al (2018) Preparation and characterization of PVA/nanocellulose/Ag nanocomposite films for antimicrobial food packaging. Carbohydrate Polymers 184:453–464. https://doi.org/10.1016/j.carbpol.2017.12.068

24. Gasti T, Hiremani VD, Kesti SS, et al (2021) Physicochemical and Antibacterial Evaluation of Poly (Vinyl Alcohol)/Guar Gum/Silver Nanocomposite Films for Food Packaging Applications. Journal of Polymers and the Environment. https://doi.org/10.1007/s10924-021-02123-4

25. Gasti T, Dixit S, Sataraddi SP, et al (2020) Physicochemical and Biological Evaluation of Different Extracts of Edible Solanum nigrum L. Leaves Incorporated Chitosan/Poly (Vinyl Alcohol) Composite Films. Journal of Polymers and the Environment. https://doi.org/10.1007/s10924-020-01832-6

26. Perumal AB, Sellamuthu PS, Nambiar RB, Sadiku ER (2018) Development of polyvinyl alcohol/chitosan bio-nanocomposite films reinforced with cellulose nanocrystals isolated from rice straw. Applied Surface Science 449:591–602. https://doi.org/10.1016/j.apsusc.2018.01.022

27. Hajji S, Salem RBS Ben, Hamdi M, et al (2017) Nanocomposite films based on chitosan–poly(vinyl alcohol) and silver nanoparticles with high antibacterial and antioxidant activities. Process Safety and Environmental Protection 111:112–121. https://doi.org/10.1016/j.psep.2017.06.018

28. Gasti T, Hiremani VD, Sataraddi SP, et al (2021) UV screening, swelling and in-vitro cytotoxicity study of novel chitosan/poly (1-vinylpyrrolidone-co-vinyl acetate) blend films. Chemical Data Collections 33:100684. https://doi.org/10.1016/j.cdc.2021.100684

29. Auras R, Harte B, Selke S (2004) An overview of polylactides as packaging materials. Macromolecular Bioscience 4:835–864. https://doi.org/10.1002/mabi.200400043

30. Kanmani P, Rhim JW (2014) Physical, mechanical and antimicrobial properties of gelatin based active nanocomposite films containing AgNPs and nanoclay. Food Hydrocolloids 35:644–652. https://doi.org/10.1016/j.foodhyd.2013.08.011

31. Salari M, Sowti Khiabani M, Rezaei Mokarram R, et al (2018) Development and evaluation of chitosan based active nanocomposite films containing bacterial cellulose nanocrystals and silver nanoparticles. Food Hydrocolloids 84:414–423. https://doi.org/10.1016/j.foodhyd.2018.05.037

32. Janani N, Zare EN, Salimi F, Makvandi P (2020) Antibacterial tragacanth gum-based nanocomposite films carrying ascorbic acid antioxidant for bioactive food packaging. Carbohydrate Polymers 247:116678. https://doi.org/10.1016/j.carbpol.2020.116678

33. Zhang X, Yang Y, Que W, Du Y (2016) Synthesis of high quality CuO nanoflakes and CuO-Au nanohybrids for superior visible light photocatalytic behavior. RSC Advances

6:81607–81613. https://doi.org/10.1039/c6ra12281g

34. Chowdhury S, Teoh YL, Ong KM, et al (2020) Poly(vinyl) alcohol crosslinked composite packaging film containing gold nanoparticles on shelf life extension of banana. Food Packaging and Shelf Life 24:100463. https://doi.org/10.1016/j.fpsl.2020.100463

35. Mallakpour S, Motirasoul F (2016) Covalent surface modification of α-MnO2 nanorods with l-valine amino acid by solvothermal strategy, preparation of PVA/α-MnO2-l-valine nanocomposite films and study of their morphology, thermal, mechanical, Pb(II) and Cd(II) adsorption properties. RSC Advances 6:62602–62611. https://doi.org/10.1039/c6ra11123h

36. Yang W, Owczarek JS, Fortunati E, et al (2016) Antioxidant and antibacterial lignin nanoparticles in polyvinyl alcohol/chitosan films for active packaging. Industrial Crops and Products 94:800–811. https://doi.org/10.1016/j.indcrop.2016.09.061

37. Zhang X, Liu W, Liu W, Qiu X (2020) High performance PVA/lignin nanocomposite films with excellent water vapor barrier and UV-shielding properties. International Journal of Biological Macromolecules 142:551–558. https://doi.org/10.1016/j.ijbiomac.2019.09.129

38. Nwabor OF, Singh S, Paosen S, et al (2020) Enhancement of food shelf life with polyvinyl alcohol-chitosan nanocomposite films from bioactive Eucalyptus leaf extracts. Food Bioscience 36:100609. https://doi.org/10.1016/j.fbio.2020.100609

39. Roohi, Bano K, Kuddus M, et al (2017) Microbial Enzymatic Degradation of Biodegradable Plastics. Current Pharmaceutical Biotechnology 18:. https://doi.org/10.2174/1389201018666170523165742

40. Gasti T, Dixit S, D'souza OJ, et al (2021) Smart biodegradable films based on chitosan/methylcellulose containing Phyllanthus reticulatus anthocyanin for monitoring the freshness of fish fillet. International Journal of Biological Macromolecules 187:451–461. https://doi.org/10.1016/j.ijbiomac.2021.07.128

41. Grosser N, Oberle S, Berndt G, et al (2004) Antioxidant action of L-alanine: Heme oxygenase-1 and ferritin as possible mediators. Biochemical and Biophysical Research Communications 314:351–355. https://doi.org/10.1016/j.bbrc.2003.12.089

42. Amin KM, Partila AM, Abd El-Rehim HA, Deghiedy NM (2020) Antimicrobial ZnO Nanoparticle–Doped Polyvinyl Alcohol/Pluronic Blends as Active Food Packaging Films. Particle and Particle Systems Characterization 37:. https://doi.org/10.1002/ppsc.202000006

43. Mathew S, Mathew J, Radhakrishnan EK (2019) Polyvinyl alcohol/silver nanocomposite films fabricated under the influence of solar radiation as effective antimicrobial food packaging material. Journal of Polymer Research 26:1–11. https://doi.org/10.1007/s10965-019-1888-0

44. Gutha Y, Pathak JL, Zhang W, et al (2017) Antibacterial and wound healing properties of chitosan/poly(vinyl alcohol)/zinc oxide beads (CS/PVA/ZnO). International Journal of Biological Macromolecules 103:234–241. https://doi.org/10.1016/j.ijbiomac.2017.05.020

45. Park GH, Kang MS, Knowles JC, Gong MS (2016) Synthesis, characterization, and biocompatible properties of alanine-grafted chitosan copolymers. Journal of Biomaterials Applications 30:1350–1361. https://doi.org/10.1177/0885328215626892

Figures

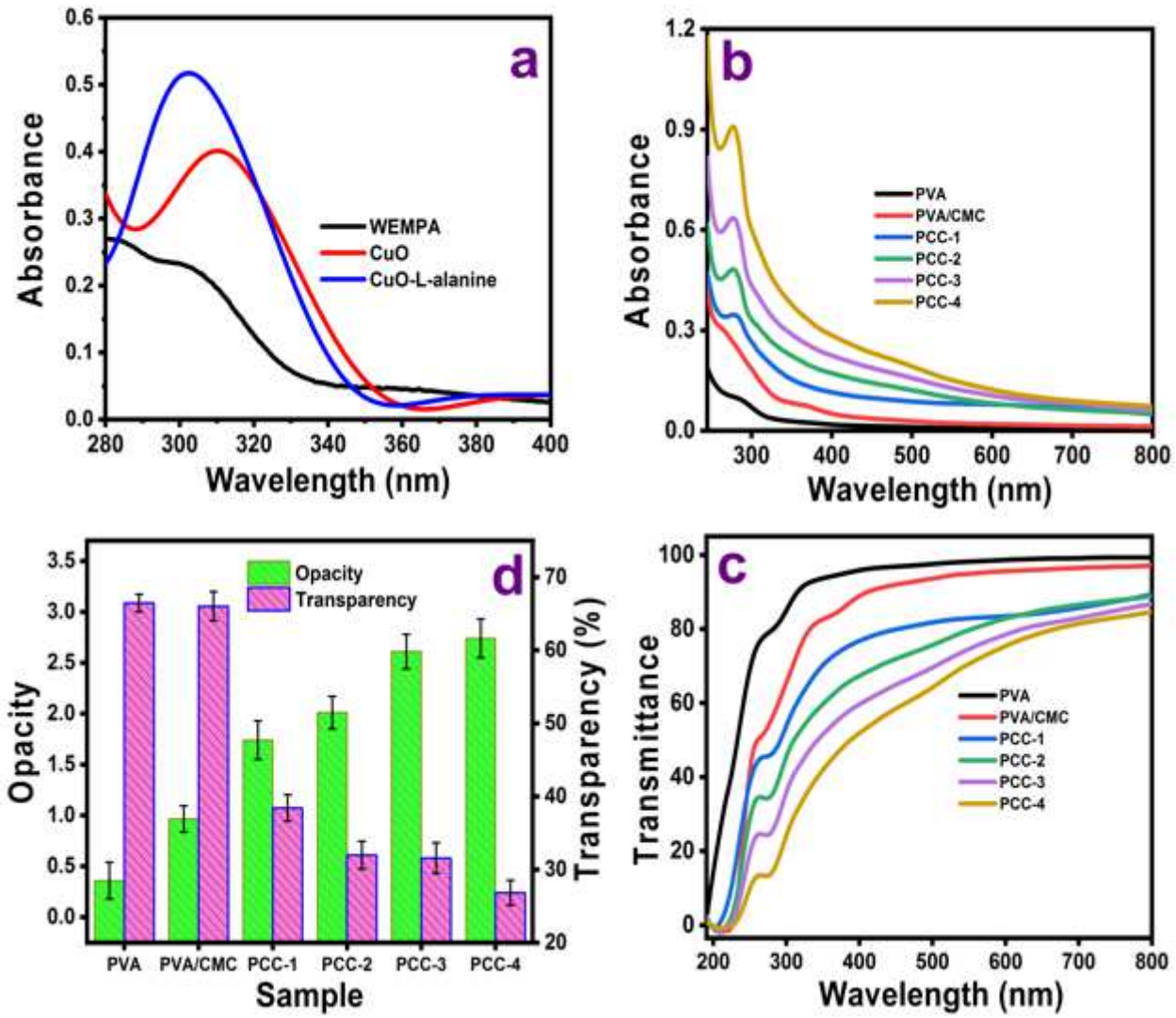

Figure 1

a) UV-Vis spectra of: A) WEMPA, B) CuO nanorods and C) CuO-L-alanine; Optical properties of the prepared films; b) UV–Vis absorption, c) % Transmittance; d) Opacity at 500 nm and Transparency at 600 nm (mean ± SD, n = 3).

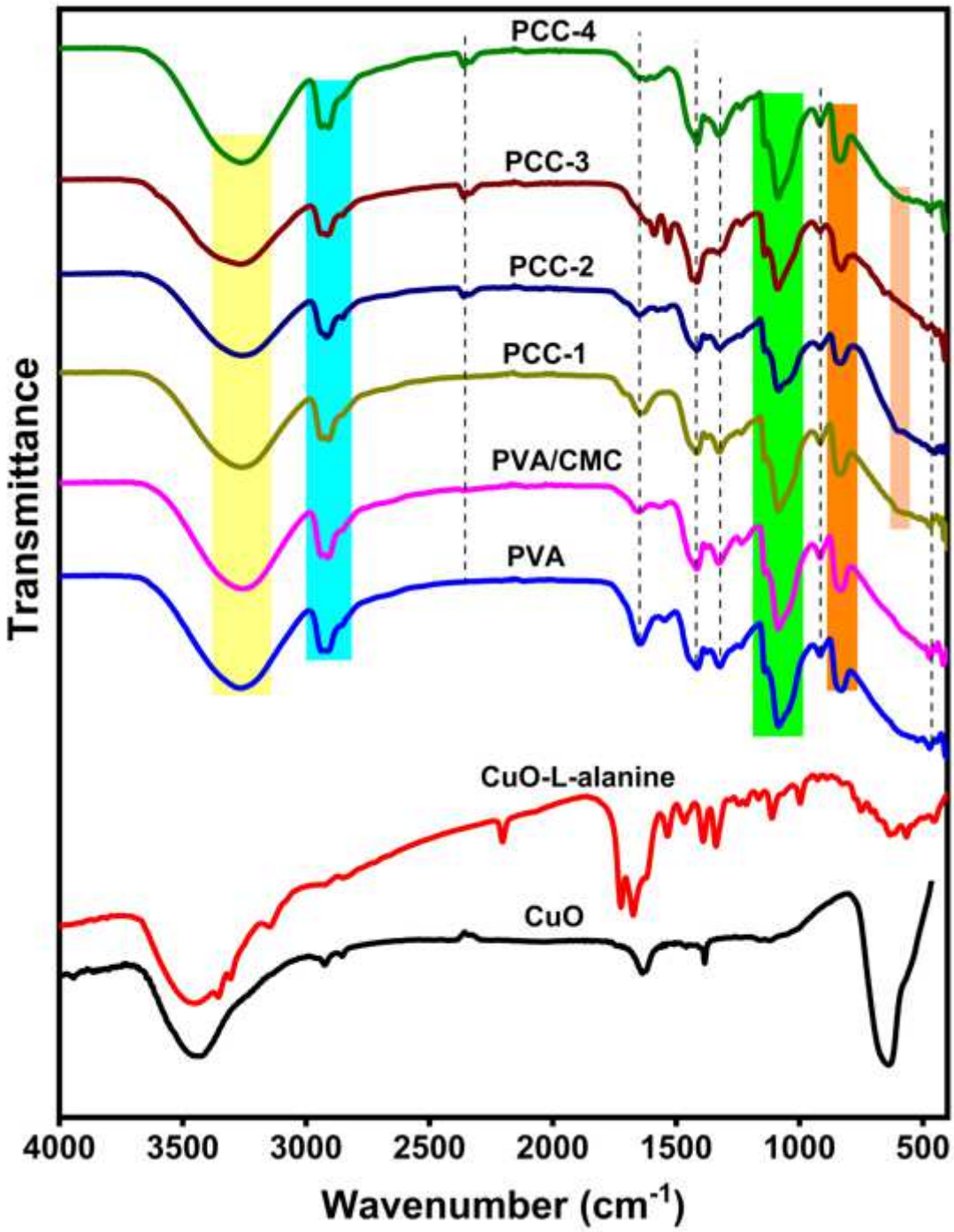

Figure 2

FT-IR spectra of CuO, CuO-L-alanine, pure PVA, PVA/CMC and NC film.

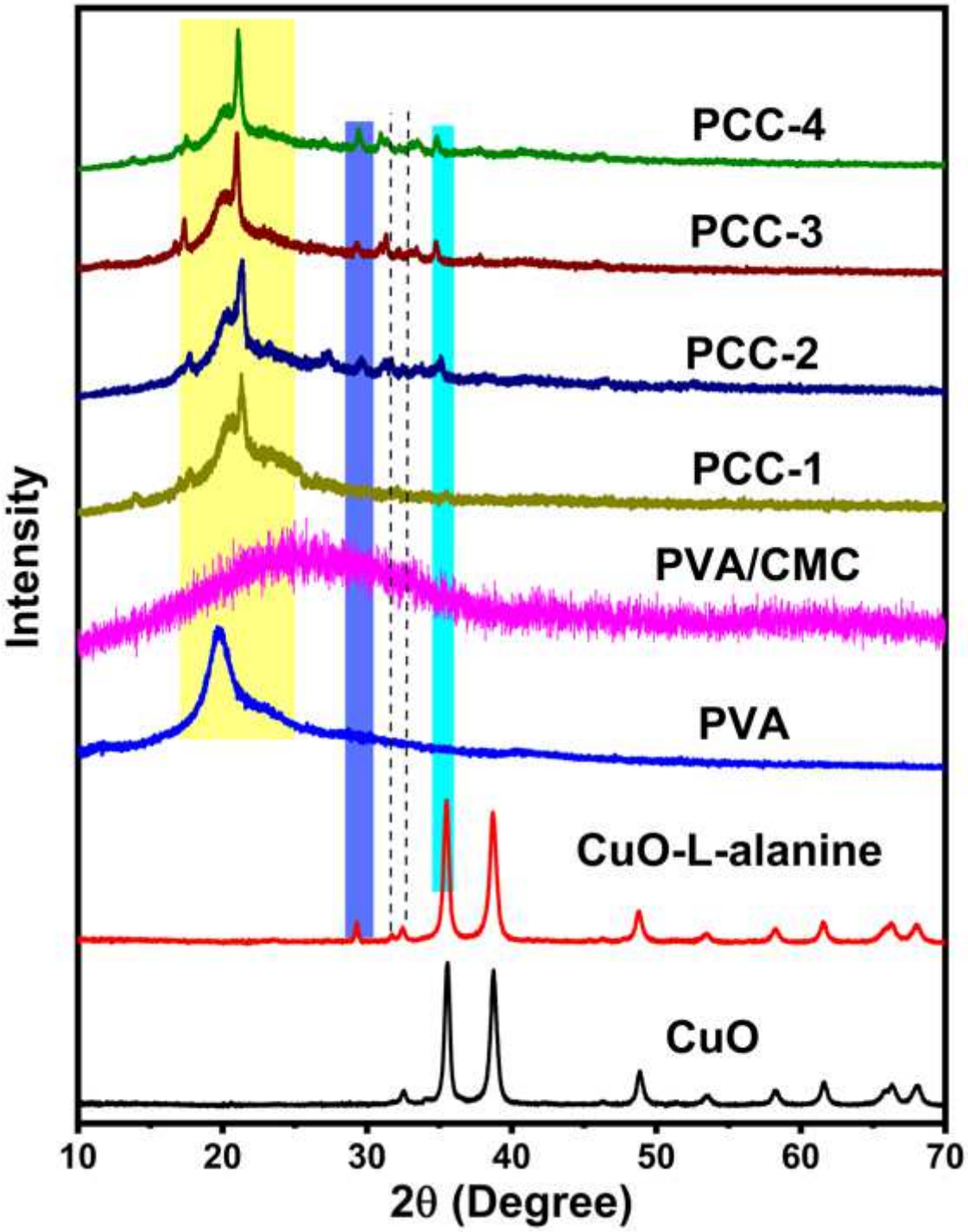

Figure 3

XRD spectra of CuO, CuO-L-alanine, pure PVA, PVA/CMC and NC films.

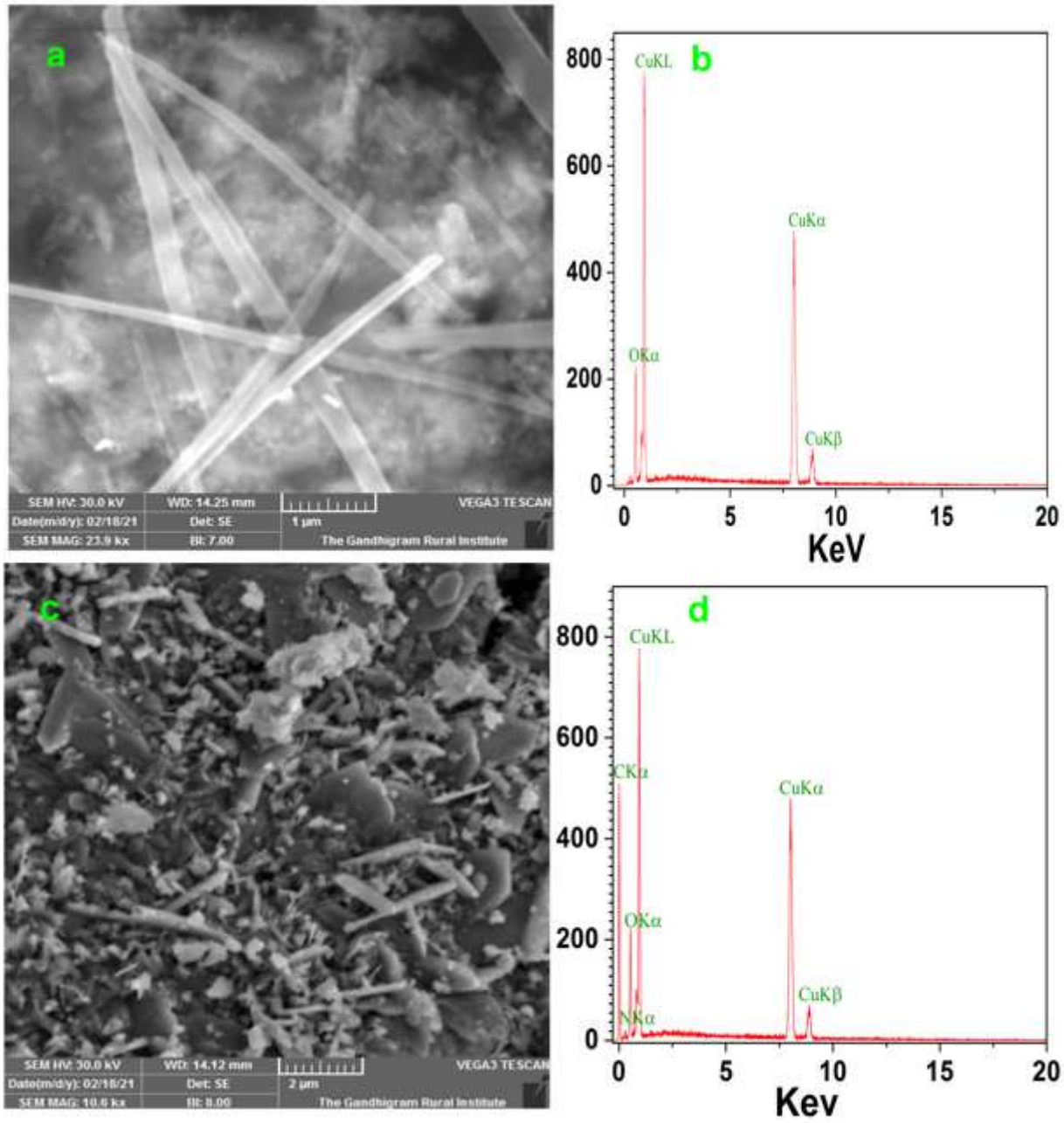

Figure 4

SEM image of CuO (a), EDX spectrum of CuO (b), SEM image of CuO-L-alanine (c), EDX spectrum of CuO-L-alanine (d).

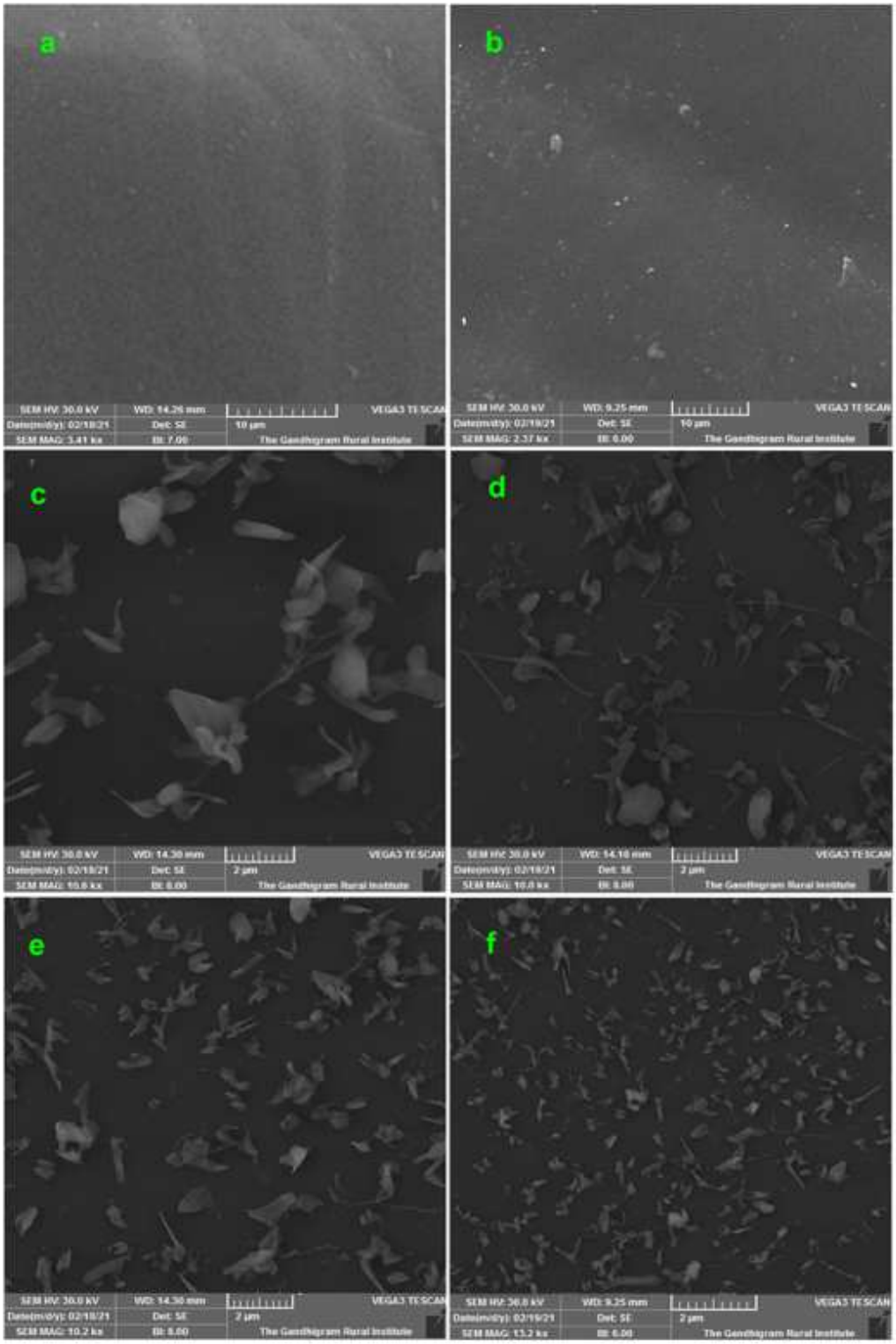

Figure 5

SEM images of PVA (a), PVA/CMC (b), PCC-1 (c), PCC-2 (d), PCC-3 (e) and PCC-4 (f).

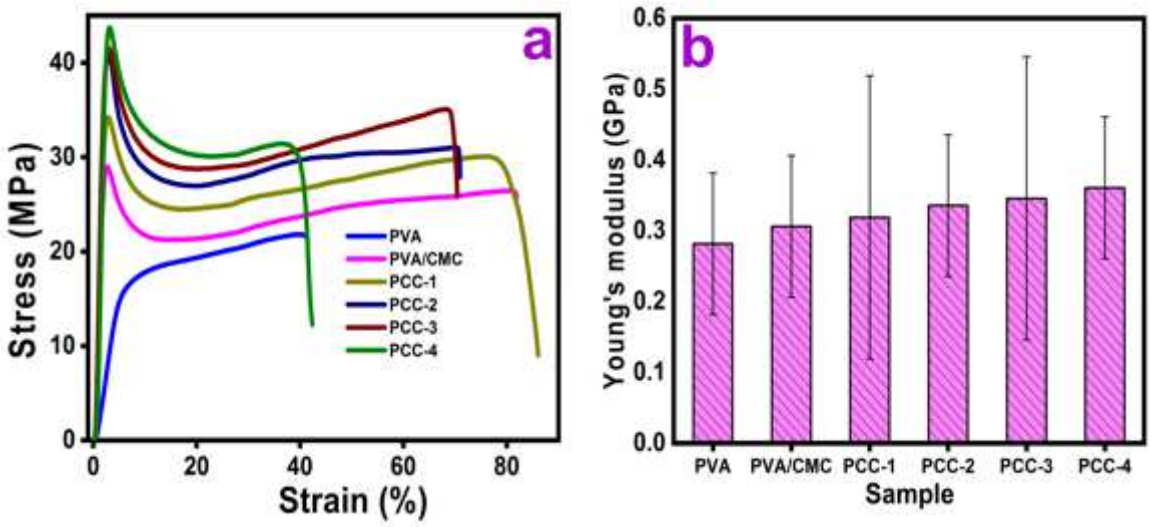

Figure 6

Breaking stress and elongation at break (a) and Young's modulus (b) of PVA, PVA/CMC and NC film (mean ± SD, n = 3).

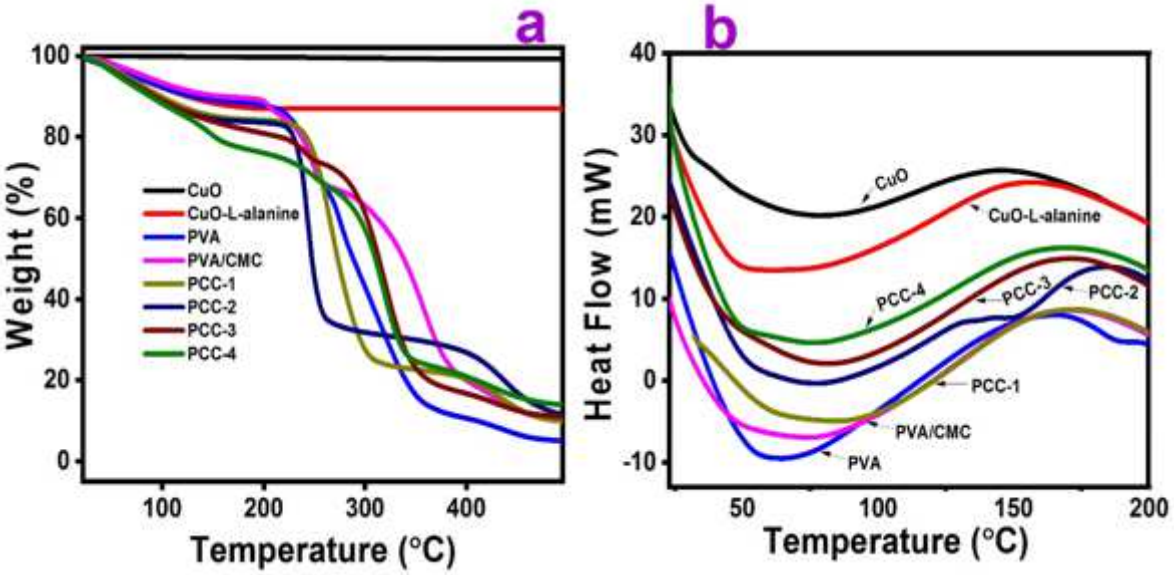

Figure 7

TGA (a) and DSC (b) curves of prepared PVA, PVA/CMC and NC films.

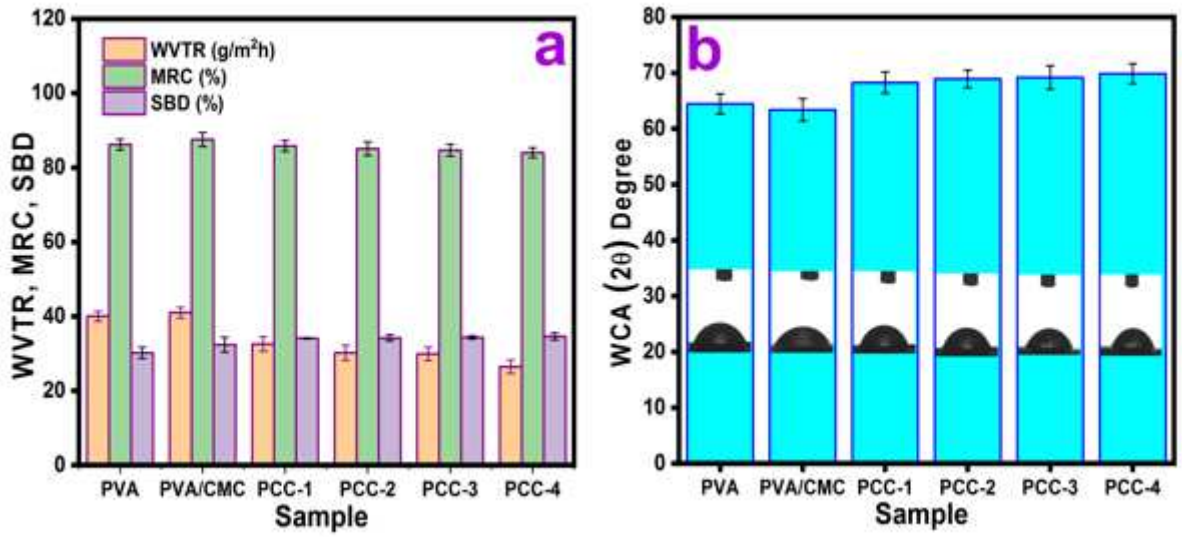

Figure 8

WVTR, MRC and Soil burial degradation (a) and WCA (b) of PVA, PVA/CMC and NC films (mean ± SD, n = 3).

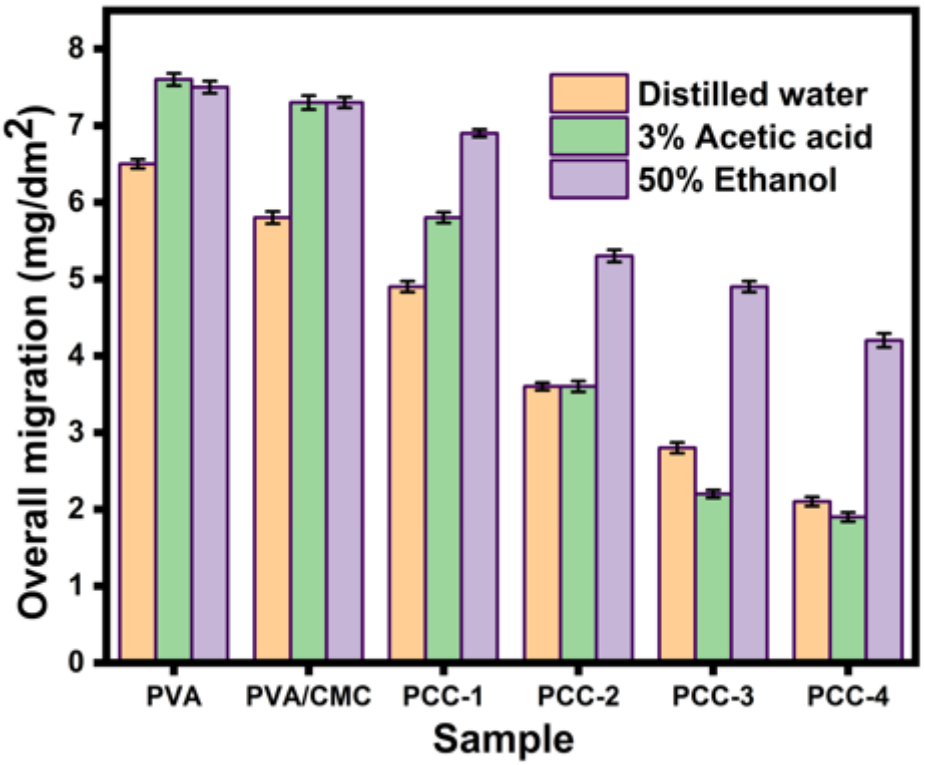

Figure 9

Overall migration rate (food compatibility) of PVA, PVA/CMC and NC films (mean ± SD, n = 3).

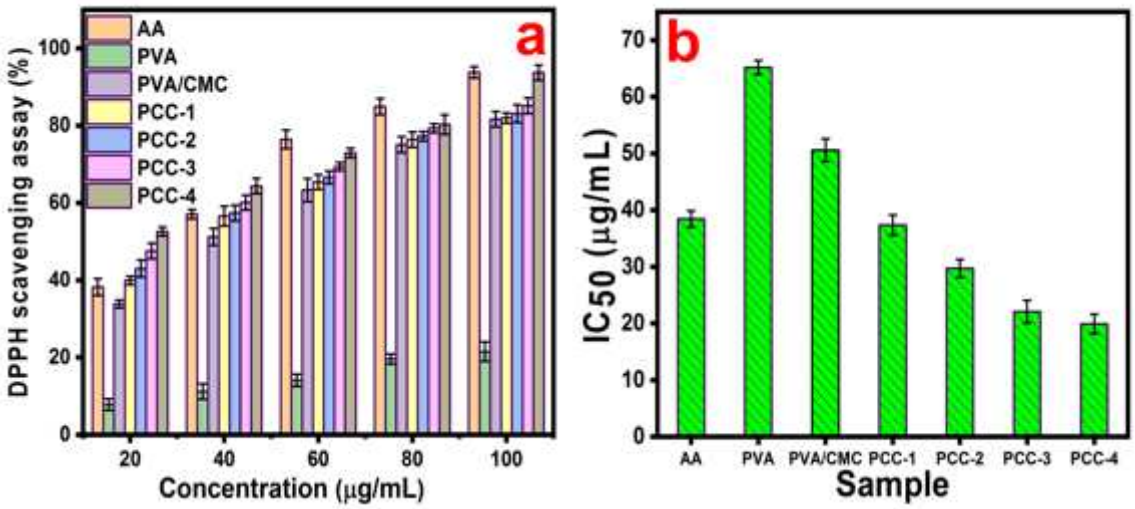

Figure 10

Antioxidant profile (a) and IC50 value of prepared PVA, PVA/CMC and NC films (b) (mean ± SD, n = 3) *AA Ascorbic acid.

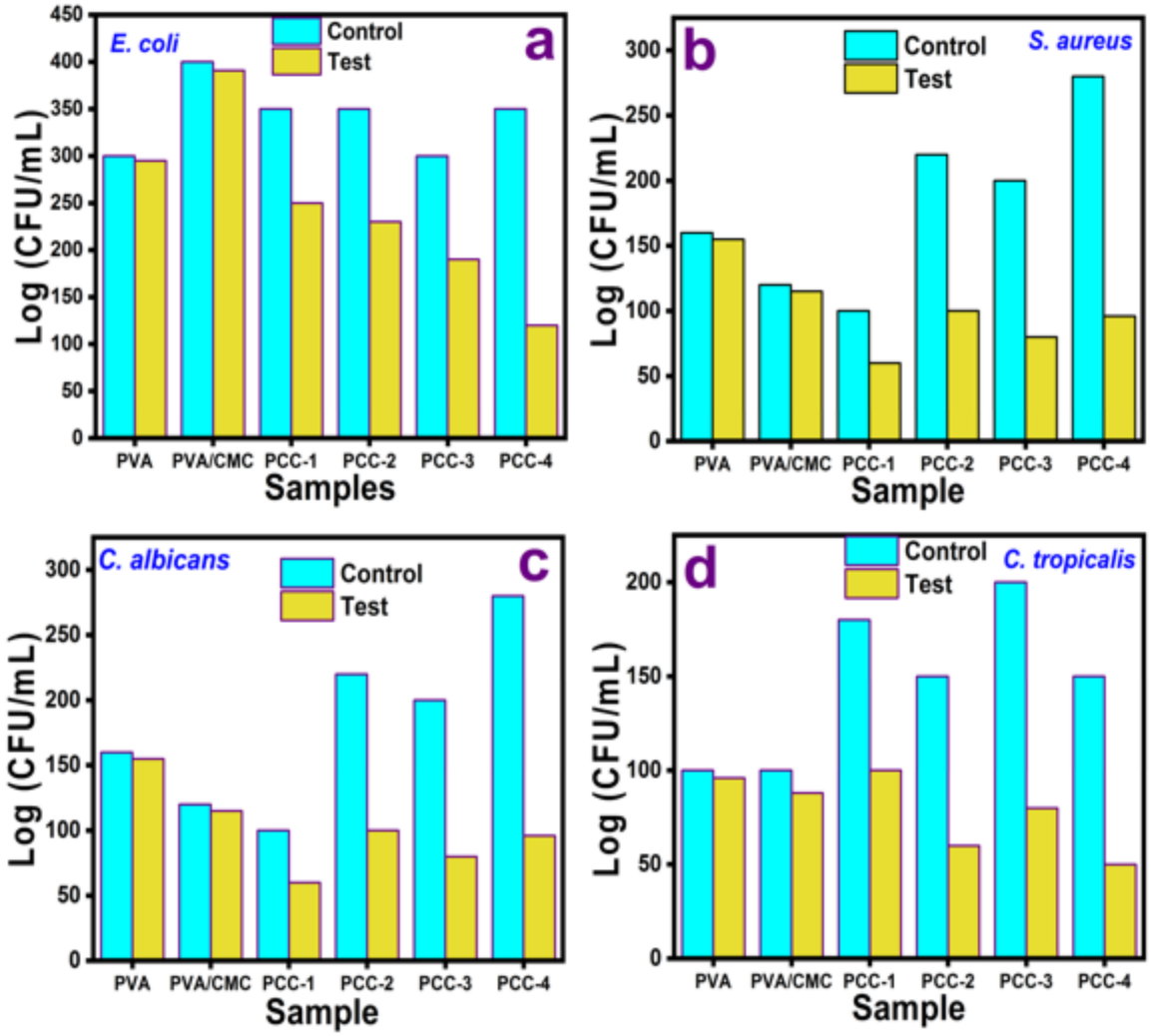

Figure 11

Log CFU/ mL of PVA, PVA/CMC and NC films against E. coli (a), S. aureus (b), C. albicans (c) and C. tropicalis (d).

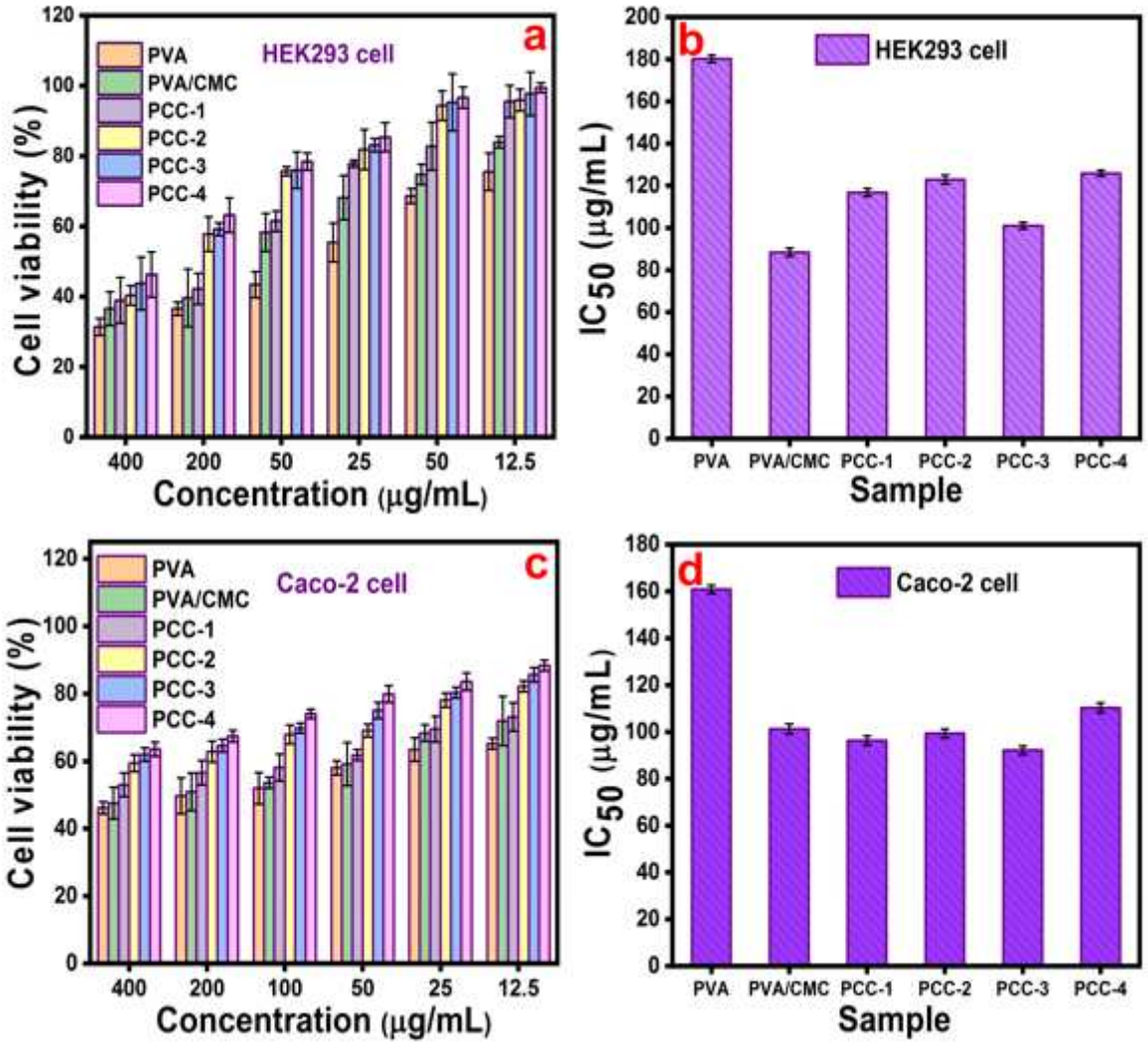

Figure 12

Effect of PVA, PVA/CMC and NC films on cell viability of HEK293 (Human embryonic kidney cell line) (a), IC50 value of HEK293 (b), Caco-2 (Cancer coli-2 cell line) (c) and IC50 value of Caco-2 cell line (mean ± SD, n = 3).

Supplementary Files

This is a list of supplementary files associated with this preprint. Click to download.

- Graphicalabstract.docx
- Electronicsupportinginformation.docx